Journal of Molecular Liquids 202 (2015) 125–133

Contents lists available at ScienceDirect

Journal of Molecular Liquids

journal homepage: www.elsevier.com/locate/molliq

New U-shaped liquid crystals azobenzene derived from catechol for photoswitching properties

Md. Lutfor Rahman [a,*], Tapan Kumar Biswas [a], Shaheen M. Sarkar [a], Mashitah Mohd Yusoff [a], Muhammad Nor Fazli Abdul Malek [a], Carsten Tschierske [b]

[a] Faculty of Industrial Sciences and Technology, Universiti Malaysia Pahang, 26300 Gambang, Kuantan, Pahang, Malaysia
[b] Institute of Organic Chemistry, Martin-Luther-University Halle-Wittenberg, Kurt-Mothes Str. 2, Halle D-06120, Germany

ARTICLE INFO

Article history:
Received 7 September 2014
Received in revised form 14 December 2014
Accepted 15 December 2014
Available online 18 December 2014

Keywords:
Azobenzene
U-shaped
Smectic phase
Isomerisation
Photoswitching

ABSTRACT

A new series of liquid crystals whose molecular structure consists of a U-shaped unit as a central core and two rod-like azobenzenes as the peripheral units are synthesized. The mesomorphic properties were investigated by differential scanning calorimetry, polarizing optical microscopy and X-ray diffraction. The existence of nematic and smectic A phase was confirmed by textures and X-ray diffraction. The *trans*-form of azo compounds showed a strong band in the UV region at ~365 nm for the π–π* transition, and a weak band in the visible region at ~450 nm due to the n–π* transition. These molecules exhibit a strong photoisomerization behavior in which *trans–cis* take 50 and 55 s for compounds L4/5 and L4/6, respectively, whereas *cis–trans* take place almost 29 and 30 h, respectively. Long thermal back relaxation allows us to realize that optical storage devices with these materials which need longer periods.

1. Introduction

In principle, the thermotropic liquid crystals (LCs) constructed by rod-like molecules exhibit nematic and/or smectic mesophases, whereas LCs with flat disc-shaped molecules display nematic and/or columnar mesophases [1,2]. A new class of LCs whose anisotropic shape of the molecules is distorted away from the classical rod or disc shapes so called 'non-conventional LCs', for instance oligomeric LCs, bent-core molecules, polycatenars, and dendrimers [1,3]. Indeed, the non-classical molecular architectures may exhibit mesophases even though their molecular geometry deviate substantially from the classical rod or disc shapes [1]. In reality, since the time of Vorlander who is famous in LCs synthesis and design, his colleague Apel [4,5] reported the first synthesis of bent-core molecules. Disubstitution of the benzene ring either 1,2 or 1,3-positions derived into U-shaped or bent-shaped molecules that deviates significantly from classical rod-shaped molecules.

Although Yelamaggad et al. [1] described that bent core V-shaped molecules of 1,2-phenylene bis[*N*-(2-hydroxy-4-*n*-alkoxyloxybenzylidene)-4′-aminobenzoate]s and other reported compounds having 1,2-subsitution of benzene ring, also termed as bent core V-shaped molecules [5–7]. However, several reports [8–11] are available on the 1,2-subsituted phenylene compounds showing U-shaped molecular architectures which are very relevant to this work. Therefore, we desire to designate the term U-shaped molecules in this paper. It is well-established that U-shaped molecules exhibit mesophases which are similar to classical calamitic LCs, whereas banana-shaped mesogens exhibit a new type of smectic phases, which are not comparable to the phases formed by calamitics [1]. U-shaped molecule, viz. 1,2-phenylene bis[4-(ethoxyphenylazoxy)benzoate] was first reported by Vorlander and Apel [5] and later Pelzl et al. [6] hence identified this compound that exhibit a nematic phase. Some reports also showed that bent-core compounds are found as fused twins [8] or U-shaped molecules [9]. A homologous series of U-shaped dimeric liquid crystals in which two mesogenic groups are connected via catechol is reported [10]. These compounds show the nematic and smectic C phases of the even members, whereas the odd members favor the nematic and smectic A phases. They discussed the transition behavior of the U-shaped compounds in terms of molecular shape [10].

Some interesting reports on new types of bent-core structure in which two mesogenic segments are connected to a benzene ring at the 1,2-positions through alkylene spacers, which are relevant to this study. In this connection, Attard and Douglass [11] reported such U-shaped dimeric liquid crystals, the benzene-1,2-di(4-carboxybenzyliedene-4′-*n*-alkylanilines) in which the spacers incorporated 3 to 6 methylene units, whilst terminal aliphatic chain lengths varied from 1 to 12 units. In the two homologous series, an odd number of methylene units in the spacer form nematic and smectic phases as a function of terminal chain length whereas an even number of methylene units in the spacer are purely smectogenic and in both series the first two homologues form only

* Corresponding author.
E-mail address: lutfor73@gmail.com (M.L. Rahman).

http://dx.doi.org/10.1016/j.molliq.2014.12.022
0167-7322/

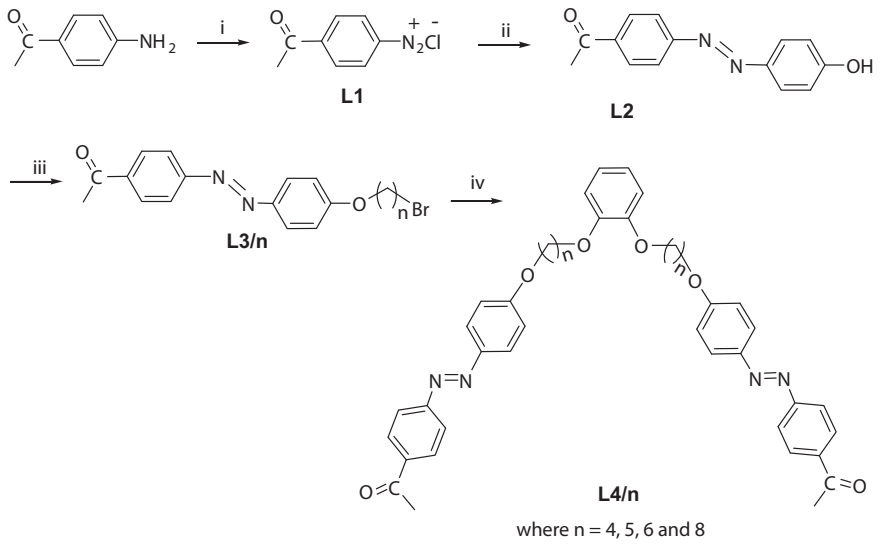

Scheme 1. Synthesis of U-shaped liquid crystals. Reagents and conditions: i, $NaNO_2$, HCl, 2 °C; ii, NaOH, C_6H_5OH; iii, K_2CO_3, KI, $Br(CH_2)_nBr$; iv, $C_6H_6O_2$ catechol, K_2CO_3.

smectic B phases. Their X-ray diffraction studies have shown that these smectic phases are composed of molecules arranged in bilayers [11].

On the other hand, a field of research is growing steadily on the photoinduced phenomenon, in which the incident light itself brings about molecular ordering/disordering of the liquid–crystalline system [12]. This particular aspect of photonics, in which light can be controlled by light as a stimulus, is being proposed as the future technology for high-speed information processing. The heart of the phenomenon in such systems is the reversible photoinduced shape transformation of the molecules containing the photochromic azo groups [13,14]. Liquid crystals having low or high molar mass containing an azo-linkage have attention due to their unique photoswitchable properties induced by light [15–19]. Upon absorption of UV light (~365 nm) the energetically more stable E configuration (*trans*) converts to the Z configuration (*cis*). The reverse transformation of the Z isomer into the E isomer can be brought by irradiation with visible light (in the range of 400 to 500 nm). This reverse process is known as thermal back relaxation which occurs in the dark and this reverse process (*cis* to the *trans*) can occur thermally or photochemically with visible light [20–27].

To the best of our knowledge, the 1,2-bis{[4-(4-acetylphenylazo) phenoxy]alkyloxy}benzene moieties have not been employed to realize such U-shaped dimeric mesogens. The introduction of flexible spacers between mesogenic units can have a profound effect on the liquid crystal properties and the phase transition behavior of U-shaped dimeric materials are related with the parities of the spacer chains and terminal alkyl chains showing nematic and smectic phases [10,11]. In this paper, we have synthesized a series of new molecules in which two rod-shaped photoswitchable azobenzene moieties, each carrying a short electron withdrawing acetyl group at the terminals [12c], are attached to a 1,2-phenylene unit via alkylene spacers and ether linkage which exhibits nematic and smectic A phases irrespective of chain length and parity.

Table 1
Phase transition temperatures (T/°C) and associated transition enthalpy values [ΔH/J g^{-1}] from the DSC scans of **L4/n** (n = 4, 5, 6 and 8).[a]

Compound	n	Heating cycles	Cooling cycles
L4/4	4	Cr 148.8 SmA 154.3 N 167.5 I [49.4] [5.0] [1.0]	I 165.4 N 151.8 SmA 82.4 Cr [1.3] [5.8] [25.9]
L4/5	5	Cr 131.3 SmA 136.8 N 149.5 I [11.1] [1.8] [0.76]	I 147.1 N 134.8 SmA 70.1 Cr [0.87] [2.3] [7.3]
L4/6	6	Cr 139.6 SmA 142.5 N 154.3 I [45.9] [2.4] [1.1]	I 152.2 N 141.1 SmA 83.6 Cr [1.3] [4.0] [31.6]
L4/8	8	Cr 135.1 SmA 138.8 N 152.4 I [32.5] [4.5] [1.0]	I 149.6 N 135.8 SmA 73.5 Cr [1.2] [4.8] [21.5]

[a] Abbreviations: Cr = crystal, SmA = smectic A, N = nematic and I = isotropic phase.

2. Characterization

The structures of the intermediates and final products were confirmed by spectroscopic methods. FT-IR spectra were recorded with a PerkinElmer (BX 20) spectrometer. ^{1}H NMR spectrum were recorded with a Jeol (ECA 600) and ^{13}C NMR was also recorded with a Jeol (150 MHz) spectrometer. The transition temperatures and their enthalpies were measured by differential scanning calorimetry (Mettler Toledo Star, SW 7.01), heating and cooling rates were 10 °C min^{-1}. Optical textures were determined by using a Mettler FP 82 hot stage and control unit in conjunction with a Nikon Optiphot 2 polarizing optical microscope. The compositions of the compounds determined by CHNS elemental analyzer (Leco & Co) confirmed molecular structures.

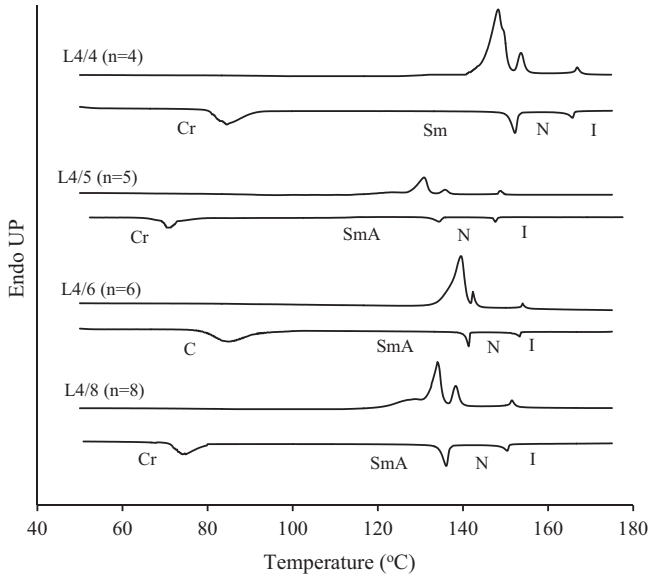

Fig. 1. DSC heating and cooling traces of compound **L4/n** (n = 4, 5, 6 and 8) at 10 °C min^{-1}.

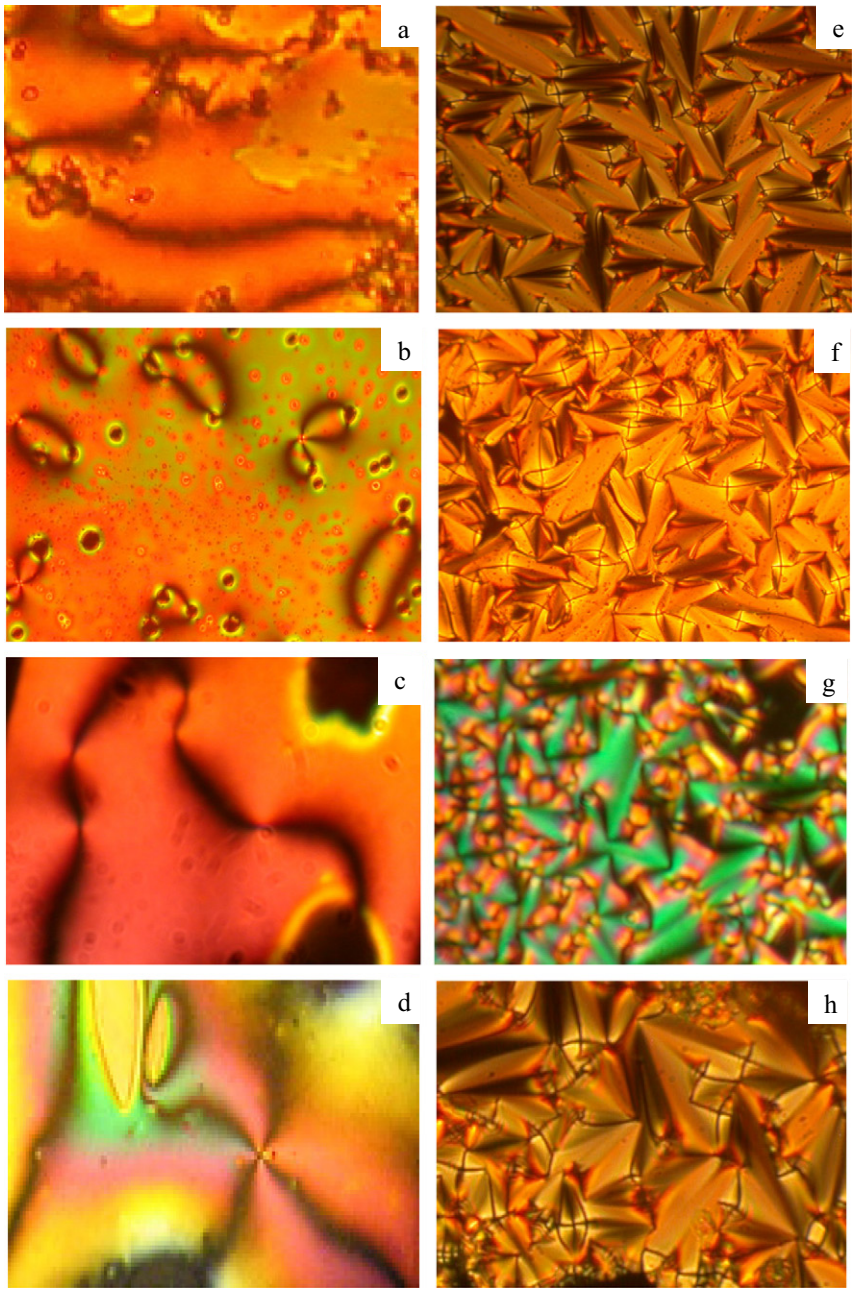

Fig. 2. Optical textures of compounds **L4/4**, **L4/5**, **L4/6** and **L4/8** on cooling from the isotropic liquids (a, b, c, d) show the nematic phases at 162, 144, 150 and 146 °C, respectively, and smectic A phases (e, f, g, h) at 145, 128, 135 and 130 °C of **L4/4**, **L4/5**, **L4/6** and **L4/8**, respectively.

X-ray diffraction measurements were carried out using Cu-Kα radiation (λ = 1.54 Å) generated from a 4 kW rotating anode generator (Rigaku Ultrax-18) equipped with a graphite crystal monochromator. Samples were filled in Hampton research capillaries (0.5 mm diameter) from isotropic phase, sealed and held on a heater. For all the samples, X-ray diffraction was carried out in the mesophase obtained on cooling of the isotropic phase and diffraction patterns were recorded on a two-dimensional image plate (Marresearch). Absorption spectra were recorded using a Shimadzu 3101 PC UV–Vis spectrometer. All the solutions were prepared and measured under air in the dark at room temperature (21 ± 1 °C) using 1 cm quartz cells. The cells were closed to avoid the evaporation of the solvent and the solutions were stirred during the irradiation time. The solutions were irradiated at $\lambda_{exc.}$ = 254 nm, 365 and 436 nm respectively, using a 200 W high pressure Hg-lamp HBO 200 (NARVA Berlin, Germany) and filters IF 254, HgMon 365, and HgMon 436 (Zeiss, Jena, Germany) generating monochromatic light as the excitation source. Additional protection glass filters Code-No 601 for irradiation at 365 nm and 254 nm and Code-No. 805 (both Schott, Jena, Germany) for irradiation at 436 nm were used.

3. Results and discussion

3.1. Synthesis

The synthetic approach used to prepare the intermediates and target compounds is outlined in Scheme 1. The peripheral rod-like side arms were prepared from 4-aminoacetophenone in which the amino group is diazotated by sodium nitrite in the acid media, the obtained diazonium salt **L1** was coupled with phenol to yield 4-(4-hydroxyphenylazo) acetophenone **L2** and purified by recrystallization from methanol with

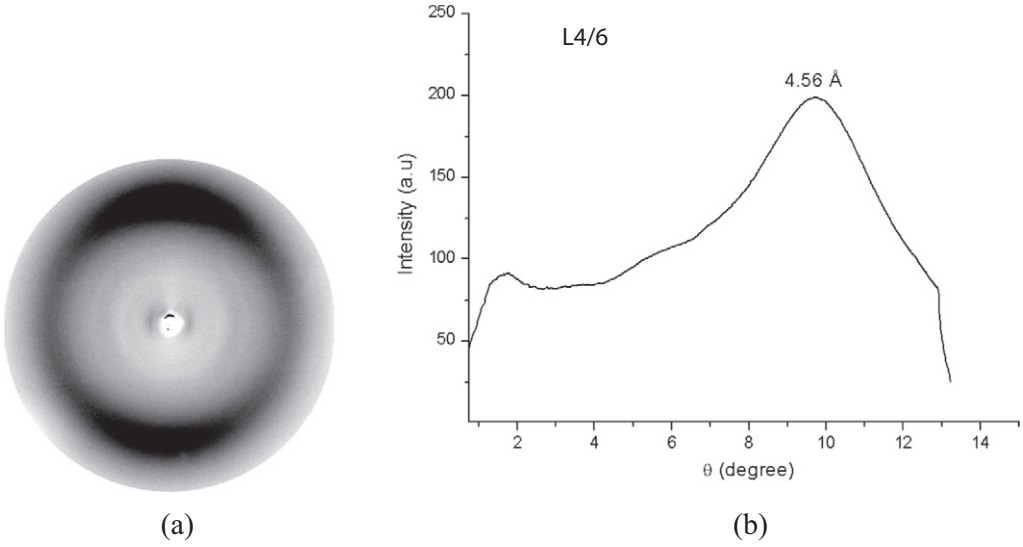

Fig. 3. (a) X-ray diffraction pattern of the compound **L4/6** at 148 °C and (b) the intensity–theta graph derived from the X-ray diffraction pattern.

58% yield. The flexible spacer was introduced by alkylation of **L2** with ten-fold excess of dibromoalkane in the presence of potassium carbonate as base to give 1-bromo[4-(4-acetylphenylazo)phenoxy]alkane **L3/n** (n = 4, 5, 6 and 8), which was purified by column chromatography on silica followed by crystallization from methanol/chloroform with 60% yield. Thus, compounds **L3/n** were used for further alkylation with catechol in the presence of potassium carbonate as base to yield the desired compounds 1,2-bis{[4-(4-acetylphenylazo)phenoxy] alkyloxy}benzene **L4/n**. All compounds were purified on silica gel by column chromatography followed by recrystallization. The synthesized compounds were characterized by ^{1}H, ^{13}C NMR and elemental analyses. Spectroscopic and analytical data were found to be in good agreement with the structures (see detailed synthetic procedures and analytical data including ^{1}H NMR spectra for **L2**, **L3/4** and **L4/4** in Supporting information).

3.2. Mesomorphic properties

The phase transition temperatures as well as the phase transition enthalpy changes were determined by differential scanning calorimetry (DSC) and the results of the second heating and cooling scans are summarized in Table 1.

The DSC thermograms of compounds **L4/n** are shown in Fig. 1. There are three peaks observed in both the endothermic and exothermic cycles for all compounds. On heating, for compound **L4/4**, these peaks appeared at 148.8, 154.3 and 167.5 °C which correspond to the Cr–SmA, SmA–N and N–I transitions, respectively. On cooling, the isotropic to nematic and nematic to smectic phase transitions occurred with minor hysteresis at 165.4 and 151.8, respectively. The compound crystallized at 82.4 °C with significant super-cooling (Fig. 1).

Similarly, compound **L4/5** exhibited three peaks on heating at 131.3, 136.8 and 149.5 °C, which correspond to the Cr–SmA, SmA–N and N–I transitions. On cooling, transitions at 147.1, 134.8 and 70.1 °C corresponding to I–N, N–SmA and SmA–Cr were observed. Compound **L4/6** displayed these transitions at 139.6, 142.5 and 154.3 °C on heating and at 152.2, 141.1 and 83.6 °C on cooling. As can be seen, these transitions occurred at a slightly lower temperature compared to **L4/4** but at a slightly higher temperature compared to **L4/5**. This could be due to the odd even effect of the spacer. Compound **L4/8**, as expected, displayed the Cr–SmA, SmA–N and N–I transitions at 135.1, 138.8 and 152.4 °C, respectively on heating. During the cooling cycle, transitions corresponding to I–N, N–SmA and SmA–Cr occurred at 149.6, 135.8 and 73.5 °C. In all the compounds (**L4/4**–**L4/8**), the crystallization from mesophase occurred with significant super cooling. The enthalpy changes for all the transitions followed the normal trend, i.e., highest for Cr–Sm transition, medium for Sm–N transition and lowest for the N–I transition. In addition, the lower alkyl chain shows a higher transition temperature, and phase transition for compound **L4/4** (n = 4) is Cr 148.8 SmA 154.3 N 167.5 I, whereas for compound **L4/8** (n = 8) it is Cr 135.1 SmA 138.8 N 152.4 I. However, the odd number of carbon atom (**L4/5**) shows lower transition temperature than any even number of carbon chains in this series.

The mesophase structures were evaluated by polarizing optical microscopy. The micrographs of the two mesophases of all compounds **L4/n** (n = 4, 5, 6 and 8) as observed upon cooling from the isotropic phase are shown in Fig. 2. All the compounds display typical schlieren texture for nematic phase upon cooling from the isotropic phase. Photomicrographs of the textures were taken at 162, 144, 150 and 146 °C for compounds **L4/4**, **L4/5**, **L4/6** and **L4/8**, respectively as shown in Fig. 2a–d. Upon further cooling a focal conic fan-like texture, typical for a smectic A phase was observed. Photomicrograph of textures were taken at 145, 128, 135 and 130 °C for compounds **L4/4**, **L4/5**, **L4/6** and **L4/8**, respectively as shown in Fig. 2e–h. The extinction crosses are parallel to polarizer and analyzer which indicate non-tilted smectic phases for all compounds **L4/n**. Upon shearing, homeotropic alignment was achieved and these homeotropically aligned regions showed complete darkness which confirmed the presence of a uniaxial SmA phases for these compounds **L4/n**.

3.3. X-ray diffraction studies

The phase structures were further characterized by X-ray diffraction analysis for a representative compound. X-ray diffraction studies confirm the phase assignment. Though a magnetic field of about 5 k Gauss was used to align the samples, the diffraction patterns indicate that the sample was not aligned perfectly and, therefore, should be considered as unaligned sample. Fig. 3(a) shows the X-ray diffraction pattern and Fig. 3(b) shows the intensity versus θ plot derived from the diffraction pattern of the compound **L4/6** at 148 °C. The X-ray pattern in the nematic phase consists of two very weak diffuse side arc-like scattering maximum in the small angle region, and a diffuse scattering in the wide angle region. The broad peak with a d-spacing of ~4.56 Å was due to the liquid-like packing of the aliphatic chains. In the smectic A phase at 130 °C, the arc spots in the small angle region

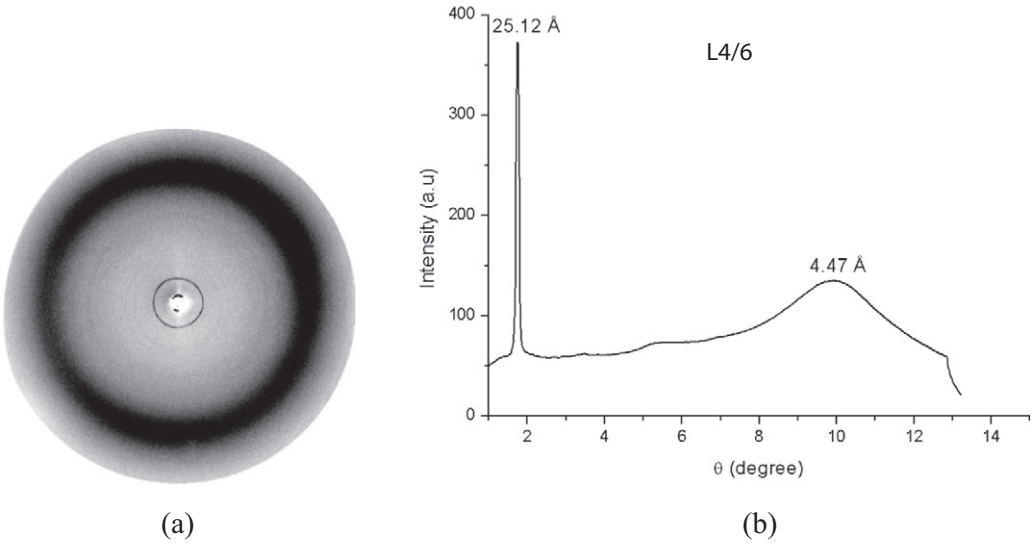

Fig. 4. (a) X-ray diffraction pattern of the compound **L4/6** at 130 °C (in the smectic A phase) and (b) the intensity-theta graph derived from the X-ray diffraction pattern.

are smeared to form a closed ring (Fig. 4a). The diffraction pattern of the SmA phase exhibited a sharp reflection in the small angle region, corresponding to d = 25.12 Å and a diffuse scattering in the wide angle region at d = 4.47 Å (Fig. 4b).

A similar pattern was obtained for sample of **L4/4** in the nematic and smectic phases. The diffraction pattern of the nematic phase is confirmed by no reflection in the small angle region and a diffuse scattering in the wide angle region, corresponding to d = 4.55 Å at 160 °C as shown in Fig. S1b and X-ray diffraction pattern shown in Fig. S1a (see in the ESI). In the smectic A phase at 140 °C, the arc spots in the small angle region are smeared to form a closed ring (Fig. S2a). The diffraction pattern of the SmA phase is characterized by a diffuse scattering in the wide angle region at d = 4.44 Å and only one sharp reflection in small angle region, corresponding to d = 22.34 Å at 140 °C (Fig. S2b).

The diffraction pattern of compound **L4/n** exhibits a sharp reflection in the small angle region, corresponding to d = 25.12 Å for **L4/6**, which is nearly equal to the molecular length of **L4/6** (length 25.5 Å) as estimated from top-to-bottom of a U-shaped conformer as shown in Fig. 5a. In the wide-angle region, a diffuse peak at d ≈ 4.47 Å, confirms a fluid smectic phase without in-plane order. Therefore, we anticipate that compound **L4/n** exhibits a smectic A type phase which is absolutely similar to compounds **L4/n**, because in case of **L4/4**, where d = 22.34 Å which is also equal to the molecular length of **L4/4** (length 22.21 Å). This is most likely due to the V-shape of the molecules **L4/n** which favors a parallel organization of the adjacent rod-like azobenzene units (thus adopting a U-shaped conformation). However, the alignment of the rod-like cores cannot be fully parallel, so that some wedge-shape (U-shaped conformation) of the molecules is retained which requires an antiparallel packing of the molecules with intercalated (mixed) aliphatic chains and azobenzene cores to optimize the space filling; the catechol groups from their own layers and separate the layers formed by the rod-like units and terminal chains, as shown in Fig. 5b. In compounds **L4/n**, the biphenylene core and peripheral azobenzenes are linked by more flexible spacers (longer, no semi rigid COO group), allowing a more easy conformational change. Thus, the rod-shaped parts could easily align parallel and form a smectic layer structure. A different packing information is obtained by X-ray diffraction from the smectic A phase formed by U-shaped compound showed a layer spacing of d = 53.4 Å, whereas the length of the molecule (l), with its alkyl chains in the all *trans* conformation, was estimated to be ≈31 Å. The ratio d/l ≈ 1.72 suggests that in this smectic A phase the molecules are ordered into bilayers [11]. However, a similar packing is observed for some compounds in which X-ray diffraction suggested that the layer spacing is about the same as the length of the molecule in a U-shaped. The XRD result suggests that the smectic phase is a monolayer structure in which molecules can exist in a U-shaped [10], which is in line with this report.

3.4. Photoswitching studies

Compound **L4/6** in chloroform: A solution concentration of 5.0×10^{-5} mol/L of **L4/6** was prepared in chloroform. The spectrum shows three absorptions with maximum absorbance at 261 nm, 365 nm ($\varepsilon = 34.940$ L mol^{-1} cm^{-1}) and 445 nm. Fig. 6a shows the spectral changes by irradiation at 365 nm. The absorbance at 365 nm decreases and after 55 s the photostationary state of a *cis–trans* mixture is reached. By irradiation at 436 nm the absorbance at 365 nm increases until a new photostationary state is reached. The photochemical back reaction by irradiation at 436 nm is shown in Fig. 6b.

Irradiation of solutions of azo compound **L4/6** at maximum absorption $\lambda_{max} = 365$ nm resulted in a fast decrease of the strong absorption band and in an increase at the long and short wavelength side of the absorption band at 365 nm (see arrows in Fig. 6a). At the photostationary state, the absorption spectrum does show three maxima at 280 nm, 325 and 450 nm and two isosbestic points at 320 and 425 nm.

Irradiation with light at $\lambda_{exc.} = 436$ nm of the same solution is induced to recover the original spectrum with the strong absorption at 365 nm (Fig. 6b). These results can be interpreted as a photoisomerization between the *trans*- and *cis*-state of the azo compound **L4/6** with the *trans* isomer absorbing at 365 nm. The return to the *trans* form can take place either by shining white light of wavelength 400–500 nm or by keeping it in dark. Once the photo stationary state is achieved by UV light, thereafter shining white light is commenced. As we increase the time of exposure of 436 nm light, *cis–trans* process begin and after 55 s almost all *cis* form is completely converted back to *trans* form. So this molecule exhibits strong photoisomerization phenomena with UV as well as with white light. It is interesting to note that UV On time and UV Off with white light take place at almost same time to reach photosaturation.

The thermal back reaction (*cis* → *trans*) is shown in Fig. 7a. After irradiation at 365 nm to photostationary state, the solution was kept in the dark and the back reaction was measured at λ = 365 nm after over 32 h (1920 min). The presence of two isosbestic points indicates the absence of side reactions. Fig. 7a shows an increase of the maximum absorbance at 365 nm and a decrease of the absorbance at 280 nm and

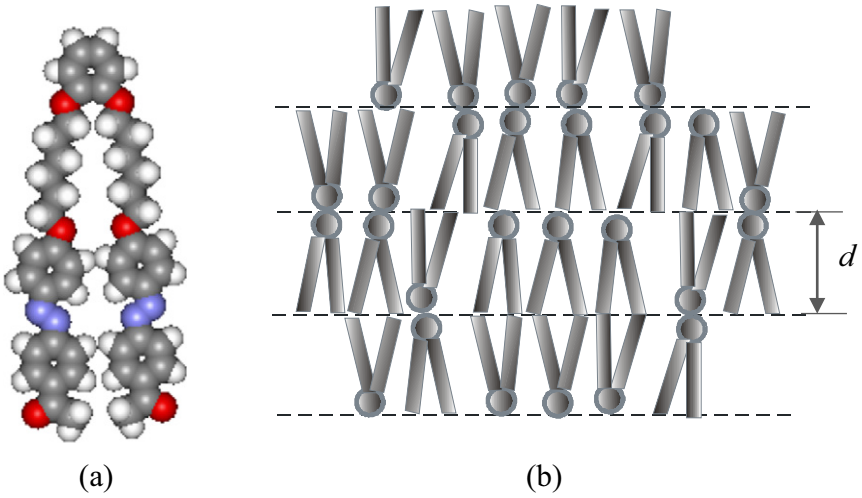

Fig. 5. (a) Major conformation of compound **L4/n** and (b) organization of these molecules in the SmA phase.

450 nm. Additionally, one can register at room temperature in the dark a thermal back reaction from the photostationary state containing mainly the *cis*-isomer to the thermodynamically more stable *trans*-isomer within the time region of 32 h. A linear correlation of ln ($E_\infty - E_t$) as a function of time indicates a reaction of first order, see Fig. 7b. After 1680 min (28 h) the conversion degree from *cis* to *trans* was 88%.

Compound **L4/6** in ethanol: For the same compound **L4/6**, the solvent is changed to ethanol instead of chloroform. The spectrum showed three absorptions at 254 nm, 365.5 nm ($\varepsilon = 34.820\ L\ mol^{-1}\ cm^{-1}$) and ~445 nm in ethanol at a concentration of 5.0×10^{-5} mol/L. The solution was irradiated at 365 nm (Fig. S3a in the ESI). The absorbance at 365 nm decreased and after 45 s the photostationary state of a *cis–trans* mixture was reached. The solution was irradiated at 436 nm until a new photostationary state is obtained and the photochemical back reaction by irradiation at 436 nm is shown in Fig. S3b (see the ESI). A fast decrease of the strong absorption band and an increase at the long and short wavelength side of the absorption band at 365 nm were observed, see arrows in Fig. S3a. The absorption spectrum at the photostationary state showed three maxima at 276 nm, 325 and 444 nm and two isosbestic points at 317 and 420 nm.

The original spectrum with the strong absorption at 365 nm was obtained by irradiation with light at $\lambda_{exc.} = 436$ nm of the same ethanol solution, see Fig. S3b. Therefore, a photoisomerization between the *trans*- and *cis*-states of the azo compound **L4/6** with the *trans* isomer absorbing at 365 nm was observed.

Thermal back reaction (*cis* → *trans*) of the **L4/6** in ethanol is presented in Fig. S4a. After irradiation at 365 nm to photostationary state, the solution was kept in the dark and the UV/Vis spectrum were measured at $\lambda = 365$ nm over 1710 min (28 h and 30 min) for converting the *cis*-isomer to the more stable *trans*-isomer within the time region of more than 28 h. The presence of the isosbestic points indicates no side reactions. Fig. S4a shows an increase of the maximum absorbance at 365 nm and a decrease of the absorbance at 276 nm and 444 nm. A plot of the ln ($E_\infty - E_t$) as a function of time is presented in Fig. S4b indicating a reaction of first order (linear correlation). After 1590 min (26 h and 30 min) the conversion of *cis* → *trans* was 96%.

Compound **L4/5** in chloroform: The spectrum in chloroform ($c = 1.2 \times 10^{-5}$ mol/L) shows three absorptions with maximum at 263.5 nm, 364 ($\varepsilon = 28.180\ l\ mol^{-1}\ cm^{-1}$) nm and a small one at about 446 nm. The solution of **L4/5** in chloroform, $c = 1.2 \times 10^{-5}$ mol/L, was irradiated with light at 365 nm (Fig. 8a). The absorbance at 365 nm decreased and the photostationary state was reached after 55 s. Irradiation of azo **L4/5** at maximum absorption $\lambda_{max} = 365$ nm has shown fast decrease of the strong absorption band and in an increase at the long and short wavelength side, see arrows in Fig. 8a. The absorption spectrum showed three maxima at 283 nm, 326 and 450 nm and two isosbestic points at 318 and 425 nm at photostationary state.

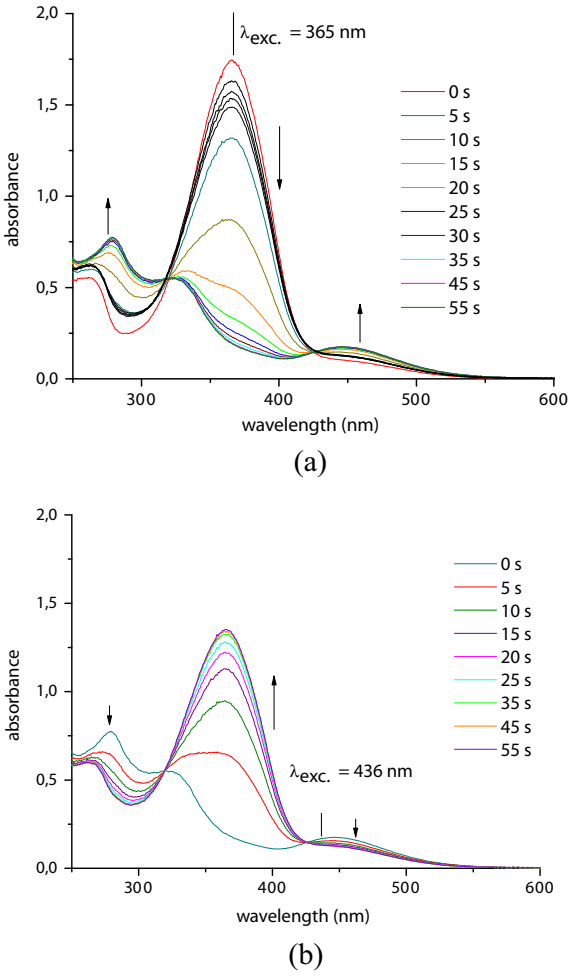

Fig. 6. UV/Vis absorption spectra of **L4/6** in chloroform, $c = 5.0 \times 10^{-5}$ mol/L, (a) irradiation at 365 nm, (b) irradiation at 436 nm (the sample was irradiated before at 365 nm).

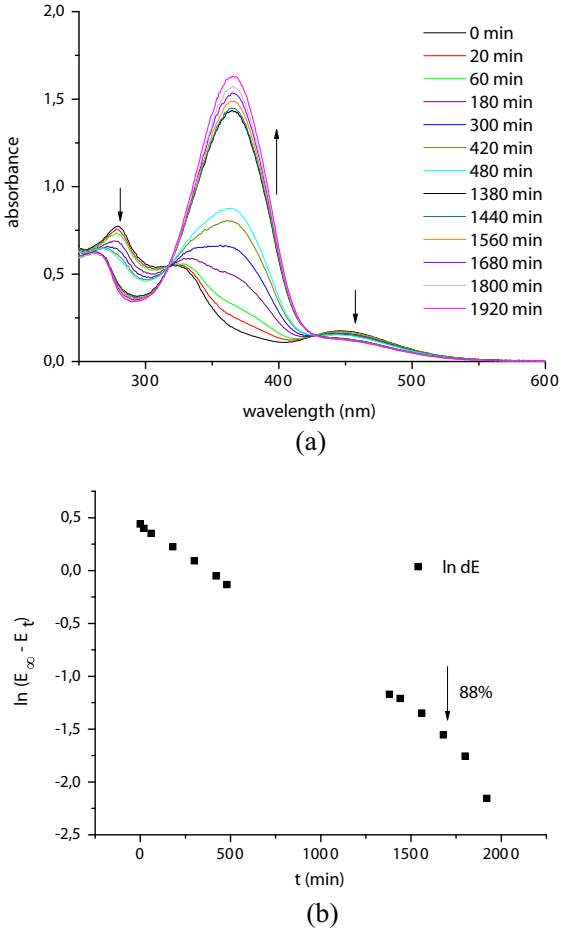

Fig. 7. (a) Thermal back reaction (*cis* → *trans*) of **L4/6** in chloroform, (b) Plot of ln ($E_\infty - E_t$) at λ = 365 nm as a function of time.

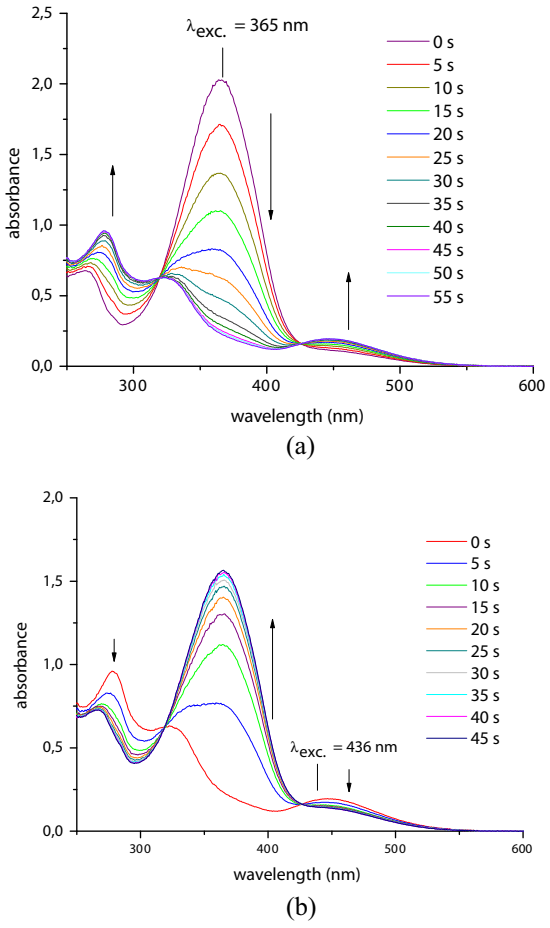

Fig. 8. UV/Vis absorption spectra of **L4/5** in chloroform after irradiation, c = 1.2×10^{-5} mol/L, (a) 365 nm, (b) 436 nm.

Fig. 8b shows the photochemical back reaction by irradiation at 436 nm in chloroform (the sample was irradiated before at 365 nm). The original spectrum was recovered with the strong absorption at 365 nm for the same solution after 45 s (see Fig. 8b).

The thermal back reaction (*cis* → *trans*) is shown in Fig. 9a. After irradiation at 365 nm to photostationary state, the back reaction was measured at λ = 365 nm over 29 h after the solution was kept in dark. The presence of the two isosbestic points indicates the absence of side reactions.

A thermal back reaction in the dark from the photostationary state, containing the *cis*-isomer is converted to the more stable *trans*-isomer within the time region of 29 h. A linear correlation of ln ($E_\infty - E_t$) as a function of time indicates a reaction of first order, see Fig. 9b. The conversion degree after 1740 min (28 h) from *cis* to *trans* was 83%.

Compound **L4/5** in ethanol: A solution of **L4/5** in ethanol at concentration of 5.0×10^{-5} mol/L was prepared in the dark. The spectrum shows two absorptions at 262 nm and 362 nm and a small one at a longer wavelength (~442 nm). The solution was irradiated at 365 nm for 5 s, up to 110 s when the photostationary state was reached (Fig. S5a). The absorption spectrum at the photostationary state shows three maxima at 277 nm, 330 and 448 nm and two isosbestic points at 320 and 420 nm. UV/Vis absorption spectra of **L4/5** in ethanol by irradiation at 254 nm and the solution were irradiated before at 365 nm for 110 s (Fig. S5b). For photochemical back reaction, a strong absorption with 365 nm of original spectrum was recovered after 450 s (Fig. S5b).

Compound **L4/6** in chloroform solution, the maximum absorbance was found at 261 nm, 365 and 445 nm. Irradiation of solutions at λ_{max} = 365 nm after 55 s at the photostationary state, three maxima were obtained at 280 nm, 325 and 450 nm. For the thermal back reaction, the *cis*-isomer to the thermodynamically more stable *trans*-isomer was converted within 32 h. The conversion degree (*cis* → *trans*) was estimated to be 88% after 28 h. Same compound **L4/6** in ethanol solution, the maximum absorbance was obtained at 254 nm, 365 and 445 nm and irradiated at λ_{max} = 365 nm after 45 s at the photostationary state, three maxima were found at 276 nm, 325 and 444 nm. For the thermal back reaction, the cis-isomer to the more stable *trans*-isomer converted within 28 h and 30 min. The conversion degree (*cis* → *trans*) was estimated to be 96% after 26 h and 30 min. The solvent effect is less pronounced in case of the UV–vis absorption before and after irradiation at 365 nm for spectral changes and also the photochemical back reaction by irradiation at 436 nm. In case of the thermal back reaction, the solvent has a substantial effect i.e., *cis* to *trans* conversion which is 96% for ethanol and 88% for chloroform.

Compound **L4/5** in chloroform solution, the maximum absorbance was at 263.5 nm, 364 and 446 nm and irradiated at 365 nm after 55 s, three maxima were observed at 283 nm, 326 and 450 nm. For the thermal back reaction, the conversion degree (*cis* → *trans*) was estimated to be 83% after 27 h. For the same compound **L4/5** in ethanol, the maximum absorbance was obtained at 262 nm, 362 and 442 nm and irradiated at 365 nm after 110 s; again three maxima were observed at 277 nm, 330 and 448 nm. Therefore, the solvent effect is less pronounced for the absorption before and after irradiation at 365 nm for spectral changes and the photochemical back reaction. A first order reaction was observed for both types of solvents and both compounds. Indeed, an almost similar behavior was observed for compounds **L4/6**

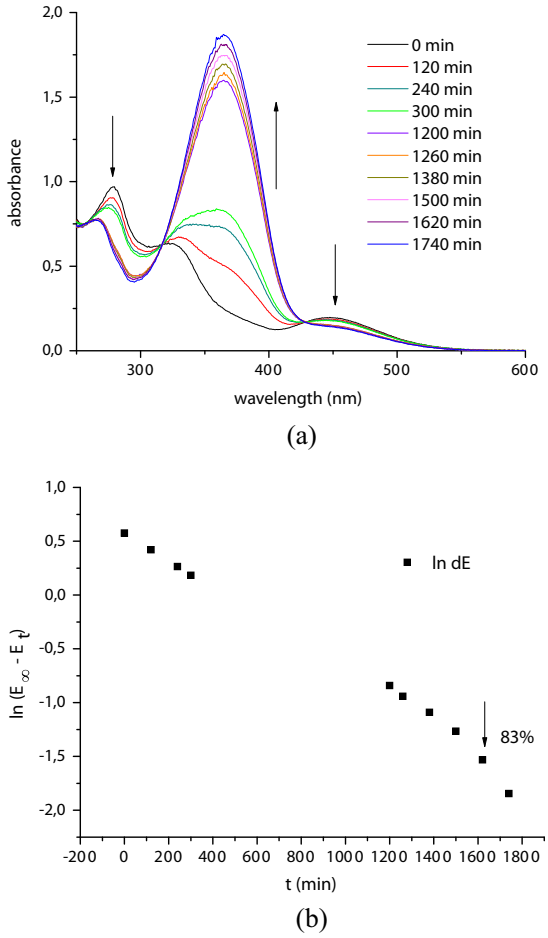

Fig. 9. Thermal back reaction (*cis* → *trans*) of **L4/5** in chloroform, (a) absorption spectra, (b) plot of ln ($E_\infty - E_t$) as a function of time.

and **L4/5** due to similar chemical structures except for one methylene group which is different in alkyl spacer.

A photostationary state from *trans* to *cis* isomer was reached within approximately 120 s under irradiation at 365 nm [22]. A photochemical switching behavior by means of cholesteric liquid crystals systems containing an azobenzene derivative as a photoisomerizable guest molecule is reported [24,25]. From the results of the investigation, the UV spectra of azo compounds in chloroform show that *trans*-azo derivatives could be changed to the *cis*-form in 70 s through UV irradiation and were found to have 12 h thermostability [25]. Muhammed et al. [23a] studied the photo-induced *cis–trans* isomerization of single azo monomer molecules in solution and the change in UV–vis absorption was monitored. The absorption relating to the π–π* transition in the trans-isomer decreases after illumination under 365 nm UV light for 45 s, and conversely, the weak absorption band due to the n–π* transition in the *cis*-isomer at 440 nm increases the absorption. They found that the *cis*-isomers of the azo monomers in solution show stability, no change was observed in the spectra for over one hour in the dark. In our previous work, the data which revealed that complete isomerization/ relaxation took place at 31 h [23b].

We have estimated the complete reaction time of *trans–cis–trans* isomerization from Figs. 6–9 including back relaxation time from first order plot. In comparison to our compounds (**L4/n**) with reported results, the spectral data are in agreement reported work. In the case of very smooth spectral changes i.e. *trans–cis–trans* isomerizations have shown good trend and smooth lines in our compounds **L4/6** and **L4/5** in both solvents. The presence of two isosbestic points indicated the absence of side reactions in our both compounds and excellent isosbestic points were observed. Indeed, our compounds showed that spectral changes which are very clear and smooth could be due to the pure dimeric U-shaped compounds derived from the catechol.

4. Conclusion

A series of new U-shaped molecules were synthesized whose molecular architecture is composed of a 1,2-phenylene unit as central core and two rod-like azobenzenes as the peripheral units linked through alkyl spacers. All the compounds show smectic A and nematic phases irrespective of chain length and parity. It seems that the phenylene unit acts only as linking unit, interconnecting the rod-like units (oligomer effect), which would lead to a smectic layer organization. Experimental study suggests that these U-shaped azo molecules exhibit strong photoisomerization properties. Very high thermal back relaxation (about 32 h) has potential advantage in the creation of optical storage devices. The presences of the azo linkage in these liquid crystals molecules are suitable for photochromism applications.

Acknowledgments

This research was supported by PRGS grant (RDU130803). We thank to the German Academy Exchange Service for a short term fellowship [code: A/03/19615].

Appendix A. Supplementary data

Supplementary data to this article can be found online at http://dx.doi.org/10.1016/j.molliq.2014.12.022.

References

[1] V.C. Yelamaggad, I. Shashikala, S.D. Rao Shankar, S.P. Krishna, Liq. Cryst. 31 (2004) 1027–1036. http://dx.doi.org/10.1080/02678290410001716015.
[2] (a) S. Chandrasekhar, Liquid Crystals, 2nd ed. Cambridge University Press, Cambridge, 1994.;
(b) G.P. Gennes De, J. Prost, The Physics of Liquid Crystals, Oxford Science Publication, Oxford, 1993.
[3] (a) C. Tschierske, J. Mater. Chem. 8 (1998) 1485–1508. http://dx.doi.org/10.1039/A800946E;
(b) C. Tschierske, J. Mater. Chem. 11 (2001) 2647–2671. http://dx.doi.org/10.1039/B102914M;
(c) C. Tschierske, Annu. Rep. Prog. Chem. C 97 (2001) 191–267. http://dx.doi.org/10.1039/B101114F;
(d) C. Tschierske, Curr. Opin. Colloid Interface Sci. 7 (2002) 69–80. http://dx.doi.org/10.1016/S1359-0294(02)00014-6.
[4] D. Vorlande, A. Apel, Ber. Dtsch. Chem. Ges. 62 (1929) 2831.
[5] D. Vorlander, A. Apel, Ber. Dtsch. Chem. Ges. 65 (1932) 1101.
[6] G. Pelzl, I. Wirth, W. Weissflog, Liq. Cryst. 28 (2001) 969–972. http://dx.doi.org/10.1080/02678290110039480.
[7] M. Kuboshita, Y. Matsunaga, H. Matsuzaki, Mol. Cryst. Liq. Cryst. 199 (1991) 319–326. http://dx.doi.org/10.1080/00268949108030943.
[8] D. Demus, Liq. Cryst. 5 (1989) 75–110. http://dx.doi.org/10.1080/02678298908026353.
[9] G. Pelzl, S. Diele, W. Weissflog, Adv. Mater. 11 (1999) 707–724. http://dx.doi.org/10.1002/(SICI)1521-4095(199906).
[10] Y. Akihisa, W. Mitsutoshi, Y. Atsushi, Liq. Cryst. 34 (2007) 633–639. http://dx.doi.org/10.1080/02678290701292355.
[11] S.G. Attard, G.A. Douglass, Liq. Cryst. 22 (1997) 349–358. http://dx.doi.org/10.1080/026782997209423.
[12] (a) R.M. Lutfor, H. Gurumurthy, Y.M. Mashitah, T.H. Srinivasa, S.A. Nurlin, M.A.M. Nor Fazli, S. Kumar, New J. Chem. 37 (2013) 2460–2467. http://dx.doi.org/10.1039/c3nj00359k;
(b) R.M. Lutfor, H. Gurumurthy, A. Mahrokh, Y.M. Mashitah, K. Sandeep, J. Fluor. Chem. 156 (2013) 230–235. http://dx.doi.org/10.1016/j.jfluchem.2013.10.004;
(c) A. Salisu, M.Z.A. Rahman, S. Silong, M.R. Lutfor, M.B.A. Ayob, Asian J. Mater. Sci. 2 (2010) 22–28.
[13] T. Sasaki, T. Ikeda, K. Ichimura, J. Am. Chem. Soc. 116 (1994) 625–628. http://dx.doi.org/10.1021/ja00081a024.
[14] (a) A. Stracke, J.H. Wendorff, D. Goldmann, D. Janietz, Liq. Cryst. 27 (2000) 1049–1057. http://dx.doi.org/10.1080/02678290050080805;
(b) M. Eich, J. Wendorff, J. Opt. Soc. Am. B 7 (1990) 1428–1436. http://dx.doi.org/10.1364/JOSAB.7.001428.
[15] T. Urbas, V. Tondiglia, L. Natarajan, R. Sutherland, H. Yu, H.J. Li, T. Bunning, J. Am. Chem. Soc. 126 (2004) 13580–13581. http://dx.doi.org/10.1021/ja045143q.

[16] K. Ichimura, K.S. Oh, M. Nakagawa, Surf. Sci. 288 (2000) 1624–1626. http://dx.doi.org/10.1126/science.288.5471.1624.
[17] L. Komitov, C. Ruslim, Y. Matsuzawa, K. Ichimura, Liq. Cryst. 27 (2000) 1011–1016. http://dx.doi.org/10.1080/02678290050080733.
[18] T. Ikeda, O. Tsutsumi, Science 268 (1995) 1873–1875. http://dx.doi.org/10.1126/science.268.5219.1873.
[19] T. Ikeda, S. Horiuchi, B.D. Karanjit, S. Kurihara, S. Tazuke, Macromolecules 23 (1990) 36–42. http://dx.doi.org/10.1021/ma00203a008.
[20] R.M. Lutfor, G. Hegde, S. Kumar, C. Tschierske, G.V. Chigrinov, Opt. Mater. 32 (2009) 176–183. http://dx.doi.org/10.1016/j.optmat.2009.07.006.
[21] T. Iked, J. Mater. Chem. 13 (2003) 2037–2057. http://dx.doi.org/10.1039/B306216N.
[22] L. Quan, L. Lanfang, K. Julie, P. Heung-shik, W. Jarrod, Chem. Mater. 17 (2005) 6018–6021. http://dx.doi.org/10.1021/cm051404z.
[23] (a) S. Muhammed, O. Jesper, T. Helena, S. Kent, K. Mikhail, Liq. Cryst. 32 (2005) 901–908. http://dx.doi.org/10.1080/02678290500139567;
(b) R.M. Lutfor, S. Kumar, S. Tschierske, G. Israel, D. Sterc, G. Hegde, Liq. Cryst. 36 (2009) 397–407. http://dx.doi.org/10.1080/02678290902923428.
[24] H.-J. Liu, C-Po Yang, K.-Y. Wang, C.-C. Wang, Liq. Cryst. 33 (2006) 237–248. http://dx.doi.org/10.1080/02678290600577971.
[25] H.-J. Liu, C-Po Yang, Liq. Cryst. 32 (2005) 539–551. http://dx.doi.org/10.1080/02678290500117654.
[26] K. Rameshbabu, P. Kannan, R. Velu, P. Ramamurthy, Liq. Cryst. 32 (2005) 823–832. http://dx.doi.org/10.1080/02678290500191261.
[27] W. Guojie, L. Min, Y. Mingming, G. Chaowei, C. Xinfang, Liq. Cryst. 27 (2000) 867–873. http://dx.doi.org/10.1080/02678290050043798.